Configurational and Conformational Aspects in the Excimer Formation of Bis(carbazoles)

J. Vandendriessche,[†] P. Palmans, S. Toppet,[†] N. Boens,[†] F. C. De Schryver,*[†] and H. Masuhara[‡]

Contribution from the Department of Chemistry, University of Leuven, Celestijnenlaan 200F, B-3030 Heverlee, Belgium, and Department of Polymer Science and Engineering, Kyoto Institute of Technology, Matsugasaki, Kyoto 606, Japan. *Received March 2, 1984*

Abstract: Intramolecular excimer formation of 1,3-di-*N*-carbazolylpropane and of *meso*- and *rac*-2,4-di-*N*-carbazolylpentane in isopentane and isooctane has been investigated. Thermodynamic and kinetic data are obtained by stationary-state and time-correlated fluorescence measurements as a function of temperature. The differences in the emission spectra are explained by considering the starting ground-state conformations as revealed by ^{1}H NMR data. *meso*-2,4-Di-*N*-carbazolylpentane has only the TG/GT conformation in the studied temperature region (180–350 K). The excimer conformation with total overlap of the chromophores (TT, λ_{max}^{em} = 420 nm) is reached via one rotation. *rac*-2,4-Di-*N*-carbazolylpentane has two conformations (TT and GG). The TT conformation of *rac*-2,4-di-*N*-carbazolylpentane is the more stable one ($\Delta G°$ = 5.1 kJ/mol) and is the precursor of the TT partial overlap excimer (λ_{max}^{em} = 370 nm). For 1,3-di-*N*-carbazolylpropane a distribution is assumed between the tt and tg$^{\pm}$ conformations. The excimer conformation (g$^{\mp}$g$^{\pm}$, λ_{max}^{em} = 420 nm) in 1,3-di-*N*-carbazolylpropane is reached via one (tg$^{\pm}$ → g$^{\mp}$g$^{\pm}$) or two rotations (tt → tg$^{\pm}$ → g$^{\mp}$g$^{\pm}$).

Spectral and dynamic aspects of intramolecular excimer formation in polymers can be studied by using bichromophoric model systems.[1-8] At first 1,3-disubstituted propanes were used as model systems,[1] but they do not reflect the specific properties of the stereochemically different dyads in the polymer. The 2,4-disubstituted pentanes are clearly a better approach, the meso and racemic isomer can be correlated respectively with the isotactic and syndiotactic dyads in the polymer.[2-8]

The emission spectrum of poly(*N*-vinylcarbazole) (PNVCz) in solution as well as in the solid state has been reported previously.[9] A broad emission band with a maximum at 420 nm has been ascribed to the emission of an excimer with total spatial overlap of the chromophores.[9] The emission band with maximum at 370 nm has long been a point of discussion. In the first report on the fluorescence of PNVCz, Klöpffer described the emission as "monomer-like" emission.[9] Johnson suggested a dimer structure with considerable deviation from coplanarity of the carbazole rings.[10] Itaya considered the conformations in the polymer chain and noted that in the TT conformation[11] of the syndiotactic chain the two carbazole groups could form a partial overlap structure.[12] This partial overlap structure is called the second excimer of PNVCz.

The fluorescence properties of the diastereoisomeric forms of 2,4-di-*N*-carabazolylpentane (*meso*- and *rac*-DNCzPe) were described in a preliminary report.[3] ^{1}H NMR data revealed the ground-state conformations of each diastereoisomer, and the differences in fluorescence properties have been explained by this information. The racemic isomer shows, besides locally excited-state emission, a structureless emission band with a maximum at 370 nm. The meso isomer shows, besides locally excited-state emission, a broad and structureless emission band with a maximum at 420 nm. Similar findings were reported in a recent paper by Evers et al.[6] Differences in spectral properties of the two diastereoisomers were reported, but no attempt was made to correlate spectral properties with starting ground-state conformations within each configuration. The transient absorption spectra of the two diastereoisomers[5] and the emission and absorption spectra of the diastereoisomers in the presence of quenchers have been reported elsewhere.[4,7]

In this paper a full description of spectral data correlated with ^{1}H NMR data on ground-state conformations is given for the diastereoisomers of 2,4-di-*N*-carabazolylpentane. The kinetics of excimer formation are interpreted taking into account the conformational restrictions. The kinetics of excimer formation in 1,3-di-*N*-carabazolylpropane (DNCzPr) are reinvestigated taking into account the two ground-state conformations and are compared with the excimer formation in the diastereoisomers.

Experimental Section

N-Isopropylcarbazole (NIPCz) and *meso*- and *rac*-2,4-di-*N*-carabazolylpentane (*meso*-DNCzPe and *rac*-DNCzPe) are the same as reported before.[3] 1,3-Di-*N*-carbazolylpropane (DNCzPr) was kindly supplied by Klöpffer, Battelle-Institut e.V., Frankfurt/Main, Germany, and was also synthesized as described in the literature.[13] *N*-Ethylcarbazole is commercially available and was purified with HPLC and TLC. The solvents were of commercially available spectrophotometric quality (Janssen) and supplementarily purified by elution through a column with silica and carbon black. The absorbance of the samples at wavelength of excitation was adjusted to 0.15. Under these experimental conditions, no intermolecular reabsorbance is observed. All solutions were degassed by several (typically four) freeze–pump–thaw cycles. The temperature of the sample was kept constant by circulating nitrogen (140–293 K), water (293–363 K), or ethylene glycol (363–393 K) through the cell holder. The temperature stability was better than 0.5 K.

Steady-state fluorescence spectra were recorded with a SPEX-fluorolog and transferred to a Digital Equipment Corporation (DEC)

(1) (a) Hirayama, F. *J. Chem. Phys.* **1965**, *42*, 3163. (b) Chandross, E. A.; Dempster, C. J. *J. Am. Chem. Soc.* **1970**, *92*, 3586. (c) Klöpffer, W. *Chem. Phys. Lett.* **1969**, *4*, 193. (d) Hara, K.; Katou, Y.; Osugi, J. *Bull. Chem. Soc. Jpn.* **1983**, *56*, 1308. (e) Zachariasse, K.; Kühnle, W. *Z. Phys. Chem.* **1976**, *101*, 267.

(2) (a) Bokobza, L.; Jasse, B.; Monnerie, L.; *Eur. Polym. J.* **1977**, *13*, 921. (b) De Schryver, F. C.; Moens, L.; Van der Auweraer, M.; Boens, N.; Monnerie, L.; Bokobza, L. *Macromolecules* **1982**, *15*, 64. (c) De Schryver, F. C.; Demeyer, K.; Van der Auweraer, M.; Quanten, E. *Ann. N. Y. Acad. Sci.* **1981**, *366*, 93. (d) Ito, S.; Yamamoto, M.; Nishijima, Y. *Bull. Chem. Soc. Jpn.* **1981**, *54*, 35.

(3) De Schryver, F. C.; Vandendriessche, J.; Toppet, S.; Demeyer, K.; Boens, N. *Macromolecules* **1982**, *15*, 406.

(4) Masuhara, H.; Vandendriessche, J.; Demeyer, K.; Boens, N.; De Schryver, F. C. *Macromolecules* **1982**, *15*, 1471.

(5) Masuhara, H.; Tamai, N.; Mataga, N.; De Schryver, F. C.; Vandendriessche, J.; Boens, N. *Chem. Phys. Lett.* **1983**, *95*, 471.

(6) Evers, F.; Kobs, K.; Memming, R.; Terrell, D. R. *J. Am. Chem. Soc.* **1983**, *105*, 5988.

(7) Masuhara, H.; Tamai, N.; Mataga, N.; De Schryver, F. C.; Vandendriessche, J. *J. Am. Chem. Soc.* **1983**, *105*, 7256.

(8) (a) Collart, P.; Demeyer, K.; Toppet, S.; De Schryver, F. C. *Macromolecules* **1983**, *16*, 1390. (b) Collart, P.; Toppet, S.; De Schryver, F. C., publication about 2,4-di-1-pyrenylpentanes in preparation for *Macromolecules*.

(9) Klöpffer, W. *J. Chem. Phys.* **1969**, *50*, 2337.

(10) Johnson, P. C.; Offen, H. W. *J. Chem. Phys.* **1971**, *55*, 2945.

(11) For the notation of the conformation in propanes, see: IUPAC, "Nomenclature of Organic Chemistry"; Pergamon Press: New York, 1979. For the notation of the conformation in pentanes, see ref 2c.

(12) Itaya, A.; Okamoto, K.; Kusubayashi, S. *Bull. Chem. Soc. Jpn.* **1976**, *49*, 2082.

(13) Lewis, I. K.; Russel, G. B.; Topsom, R. D.; Vaugham, J. *J. Org. Chem.* **1964**, *29*, 1183.

0002-7863/84/1506-8057$01.50/0

Table I. ^{1}H NMR Data of *rac*-DNCzPe in Deuterated Octane at Different Temperatures

δ	multiplicity	groups of protons	J, Hz
		T = 253 K	
1.50	d	CH_3	^3J = 7.00
3.15	*AA'*XX'	CH_2	$^2J_{AA'}$ = −15.00
			$^3J_{AX}$ = 11.84
			$^3J'_{AX}$ = 3.59
			$^4J_{XX'}$ <<ose 0
4.39	AA'*XX'*xq	CH	
5.88	d × t	H_1	^3J = 8.2[a]
			^4J < 1.0
6.61	t × d	H_2	^3J = 7.5
			^4J = 1.2
6.89	t × d	H_3	^3J = 7.5
			^4J < 1.0
7.21	t × d	H_6	^3J = 7.5
			^4J < 1.0
7.39	t × d	H_7	^3J = 7.75
			^4J = 1.2
7.62	d	H_8	^3J = 8.0
7.88	d × t	H_5	^3J = 7.75
8.09	d × t	H_4	^3J = 7.75
		T = 393 K	
1.50	d	CH_3	^3J = 7.0
3.14	*AA'*XX'	CH_2	$^2J_{AA'}$ = −15.0
			$^3J_{AX}$ = 11.00
			$^3J_{AX'}$ = 4.26
			$^1J_{XX'}$ = 0
4.51	AA'*XX'*xq	CH	
6.85		H_1, H_2	
		H_3, H_6	
7.05	m	H_7, H_8	
7.95	m	H_4, H_5	

[a] H_1–H_8: aromatic protons in position 1–8.

PDP 11/23 computer for data analysis. Fluorescence decay curves were obtained with a frequency-doubled Spectra-Physics (Models 165, 344b, 375, 452a, 454) picosecond synchronously pumped mode-locked cavity dumped dye laser (Rhodamine 6G dye). The repetition frequency was 800 kHz. An Inrad Model 563-1117 KDP"B" Crystal was used for frequency doubling. In emission a Carl Lambrecht MUG TS 10 (angle 54°44') polarizer, a monochromator, and a photomultiplier (Phillips XP2020Q) were used. The full width at half-maximum of the overall excitation pulse was 300 ps.[14] Data collection was stopped when the number of counts of emitted photons at the maximum reached 3×10^4 counts. The collected data were transferred to a DEC PDP 11/23 computer for data analysis. The experimental data were fitted to theoretical decay functions using a nonlinear least-squares decay-fitting program.[15] Five criteria were used to judge the goodness of fit:[16] chi-square (χ^2), the weighted residuals (R_i), the autocorrelation function (C_i),[17] the serial correlation function (D),[18] and the heteroscedasticity test[19] (a plot of R_i vs. $\hat{Y}_i$). A decay-fitting result was rejected when one of these parameters, or one of the plots, was not acceptable. The experimental fluorescence decay curves were analyzed with trial decay functions (eq 1) containing

$$I(t) = \sum_{i=1}^{n} A_i \exp(-\lambda_i t) \qquad (1)$$

one, two, or three exponential decaying terms. $I(t)$ is the fluorescence decay function; n = 1, 2, 3; A_i is the preexponential factor; $1/\lambda_i$ is the decay parameter. ^{1}H NMR measurements were done with a Bruker WM250 (250 MHz).

(14) Van den Zegel, M.; Boens, N.; De Schryver, F. C., unpublished results.
(15) (a) McKinnon, A. E.; Szabo, A. G.; Miller, D. R. *J. Phys. Chem.* **1977**, *81*, 1564. (b) O'Connor, D. V.; Ware, W. R.; Andre, J. C. *J. Phys. Chem.* **1979**, *83*, 1333. (c) Marquardt, D. W. *J. Soc. Indust. Appl. Math.* **1963**, *11*, 431.
(16) Roberts, A. J.; Phillips, D.; Abdul Rasoul, F. A. M.; Ledwith, A. *J. Chem. Soc., Faraday Trans. 1* **1981**, *77*, 2725.
(17) (a) Easter, J. H.; DeToma, R. P.; Brand, L. *Biophys. J.* **1976**, *16*, 571. (b) Grinvald, A.; Steinberg, J. Z. *Anal. Biochem.* **1974**, *59*, 583.
(18) (a) Durbin, J.; Watson, G. S. *Biometrika* **1950**, *37*, 409. (b) Durbin, J.; Watson, G. S. *Biometrika* **1951**, *38*, 159.
(19) Boens, N.; Van den Zegel, M.; De Schryver, F. C. *Chem. Phys. Lett.*, in press.

Table II. Conformational Distribution of *rac*-DNCzPe in Deuterated Octane, Obtained from ^{1}H NMR Measurements

T, K	TT, %	GG, %	ΔG°, kJ/mol
253	91	9	4.9
273	89	11	4.8
298	88.5	11.5	5.0
323	88	12	5.2
393	84	16	5.4

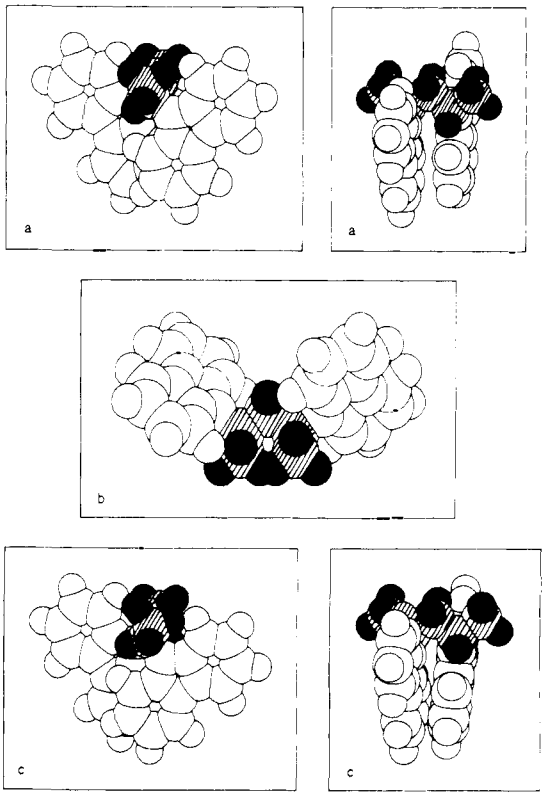

Figure 1. Space-filling models of the ground- and excited-state conformations of *rac*-DNCzPe in solution. (a) TT ground and locally excited state conformation. (b) GG ground and locally excited state conformation. (c) TT second excimer conformation.

Results and Discussion

1. ^{1}H NMR Data and the Conformational Distributions. The ^{1}H NMR data of *rac*-DNCzPe in deuterated octane at different temperatures are reported in Table I. The methylene group is homosteric, the same shift is observed for both protons. The methylene protons are analyzed as the AA' part of an AA'XX' spectrum. It was possible to calculate the ground-state conformational distribution at every temperature analogous to the calculations on the ^{1}H NMR spectra of 2,4-disubstituted pentanes reported by Bovey[20] (Table II). The main contributors to the ^{1}H NMR spectrum of a *rac*-2,4-disubstituted pentane are the TT and the GG conformation. Space-filling models of these conformations of *rac*-DNCzPe are presented in Figure 1. When the temperature is lowered an important splitting of the shift of the aromatic protons is observed. This is due to the slow rotation of the carbazole chromophores. However, the extent of the splitting is much larger than the effect reported for N1PCz.[3,21] This is explained by the influence of the ring current of the first chromophore on the protons of a part of the second chromophore and vice versa. Such a condition is fulfilled in the TT conformation (Figure 1a). The effect of the ring current will be larger for the

(20) (a) Bovey, F. A.; Hood, F. P.; Anderson, E. W.; Snyder, L. C. *Chem. Phys.* **1965**, *42*, 3900. (b) Bovey, F. A. "High Resolution NMR of Macromolecules"; Academic Press: New York, 1972; Chapter IX, pp 182–204.
(21) Hindered rotation of the carbazole chromophores in poly(*N*-vinylcarbazole) was observed: Williams, D. J. *Macromolecules* **1970**, *3*, 602.

Table III. ^{1}H NMR Data of *meso*-DNCzPe in Deuterated Octane at Different Temperatures

δ	multiplicity	group of protons	J, Hz
	T = 296 K		
1.65	d	CH_3	^3J = 7.0
2.76 (A)	ABX_2	H_ACH_B	^2J = −14.17
			$^3J_{AX}$ = 7.98
			$^3J_{BX}$ = 8.08
4.60	ABX_2, q	CH	$\overline{^3J}$ = 7.32
7.03–7.18	m	*a*	
7.95	d	*b*	^3J = 7.5
	T = 393 K		
1.65	d	CH_3	^3J = 6.98
2.73 (A)	ABX_2	H_ACH_B	^2J = −14.10
			$^3J_{AX}$ = 7.95
			$^3J_{BX}$ = 7.31
4.65	ABX_2, q	CH	$\overline{^3J}$ = 7.20
7.00–7.16	m	*a*	
7.92	d × t	*b*	^3J = 7.5
			^4J = 1.1

[a] Protons in positions 1, 2, 3, 6, 7, and 8 on the carbazole chromophores. [b] Protons in positions 4 and 5 on the carbazole chromophores.

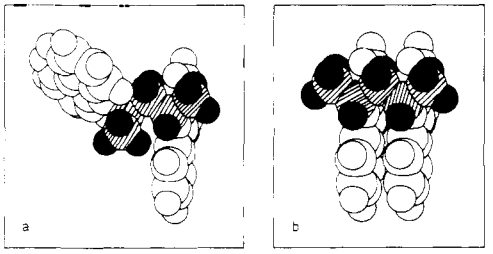

Figure 2. Space-filling models of the ground- and excited-state conformations of *meso*-DNCzPe in solution. (a) TG/GT ground and locally excited state conformation. (b) TT "normal" excimer conformation.

protons in position 1 on the carbazole ring than for protons in position 2, 3, and 4 (Table I). For symmetry reasons eight signals will be observed in the ^{1}H NMR spectrum of the aromatic protons for the TT conformation. If the GG conformation would be the more stable conformation the observed effect at low temperatures should be comparable to that of NIPCz. However, there is no indication of a stabilizing interaction of the two chromophores in the ground state of the TT conformation since no indication of a new band, a splitting of an absorption band, or even a shift of the maxima was found in the absorption spectrum *rac*-DNCzPe.[3]

The ^{1}H NMR data of *meso*-DNCzPe in deuterated octane at different temperatures are reported in Table III. The methylene group is heterosteric in the meso-2,4-disubstituted pentanes, the methylene protons have a different shift. The methylene protons are analyzed as the AB part of an ABX_2 spectrum. On the basis of considerations concerning steric hindrance and ^3J coupling constants it can be proposed that the TG/GT conformation is the most stable conformation.[20] Since $^3J_{AX} = {}^3J_{BX}$ at room temperature it is concluded that 100% of the molecules are present in the TG/GT conformation in an alkane solvent at room temperature. A space-filling model of this TG conformation is presented in Figure 2a. At 393 K a small deviation from the equality $^3J_{AX} = {}^3J_{BX}$ is observed. This could be an indication of the presence of other ground-state conformations (TT), but even at that temperature about 94% of the molecules are in the TG conformation. At lower temperatures a splitting of the aromatic part of the spectrum is observed. However, the extent of the splitting is smaller than the extent of the splitting reported for *rac*-DNCzPe and comparable to the one reported for NIPCz. The coalescence temperature is situated above 273 and below 293 K. It is concluded that the rotation of the carbazole chromophores is slow compared with photophysical processes. This fact is not very important for chromophores where a symmetry axis is present in the chromophore parallel to the bond of the chromophore with the chain (N-substituted carbazole, phenyl, ...), but it proves the necessity of considering rotamers when the photophysics of compounds such as di-2,4-pyrenylalkanes are studied.[8]

Table IV. ^{1}H NMR Data of DNCzPr in Deuterated Octane at Different Temperatures

δ	multiplicity	groups of protons	J, Hz
	T = 333 K		
2.42	quintet	CCH_2C	$\overline{^3J}$ = 7.21
4.24	t	CH_2N	$\overline{^3J}$ = 7.25
7.03–7.28	m	*a*	
7.98	d	*b*	^3J = 8.0
	T = 393 K		
2.46	quintet	CCH_2C	$\overline{^3J}$ = 7.20
4.27	t	CCH_2N	$\overline{^3J}$ = 7.64
7.05–7.29	m	*a*	
7.98	d × t	*b*	^3J = 7.5
			^4J < 1.0

[a] Protons in positions 1, 2, 3, 6, 7, and 8 on the carbazole chromophores. [b] Protons in positions 4 and 5 on the carbazole chromophores.

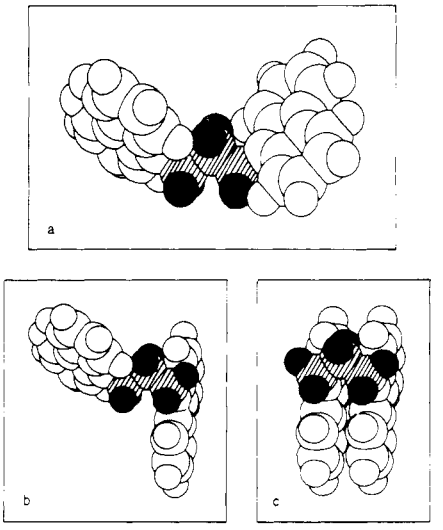

Figure 3. Space-filling models of the ground- and excited-state conformations of DNCzPr in solution. (a) tt ground and locally excited state conformation. (b) $tg^{\pm}$ ground and locally excited state conformation. (c) $g^{\mp}g^{\pm}$ excimer conformation.

The ^{1}H NMR data of DNCzPr in deuterated octane are reported in Table IV. It was not possible to obtain information about the ground-state conformational distribution in DNCzPr in solution from the ^{1}H NMR measurements. The dominant ground-state conformations of a 1,3-disubstituted propane are the tt and $tg^{\pm}$ conformations.[22] Space-filling models of these conformations for DNCzPr are presented in Figure 3a,b.

2. Emission Spectra. (a) Photostationary Measurements. The fluorescence spectrum of *rac*-DNCzPe at room temperature in isopentane is shown in Figure 4a. The emission spectrum consists of maxima at 347 and 365 nm and a shoulder at 370 nm. When the (0,0) band of the *rac*-DNCzPe emission spectrum is normalized to the (0,0) band of the NIPCz emission spectrum, a structureless band is resolved with a maximum at 370 nm. This emission is ascribed to the emission from a partial overlap excimer, the so-called second excimer.[23]

The fluorescence spectrum of *rac*-DNCzPe in an alkane solvent as a function of temperature changes as follows. At low temperatures, but still in solution (isopentane 140 K), the emission spectrum consists of nearly only excimer fluorescence (Figure 4). When the temperature is raised an increase of the emission at 347 nm is observed, and at higher temperatures a peak is resolved.

(22) Orville-Thomas, W. J., Ed. "Internal rotation in Molecules"; Wiley: London, 1974.
(23) Johnson, G. E. *J. Chem. Phys.* **1975**, *62*, 4697.

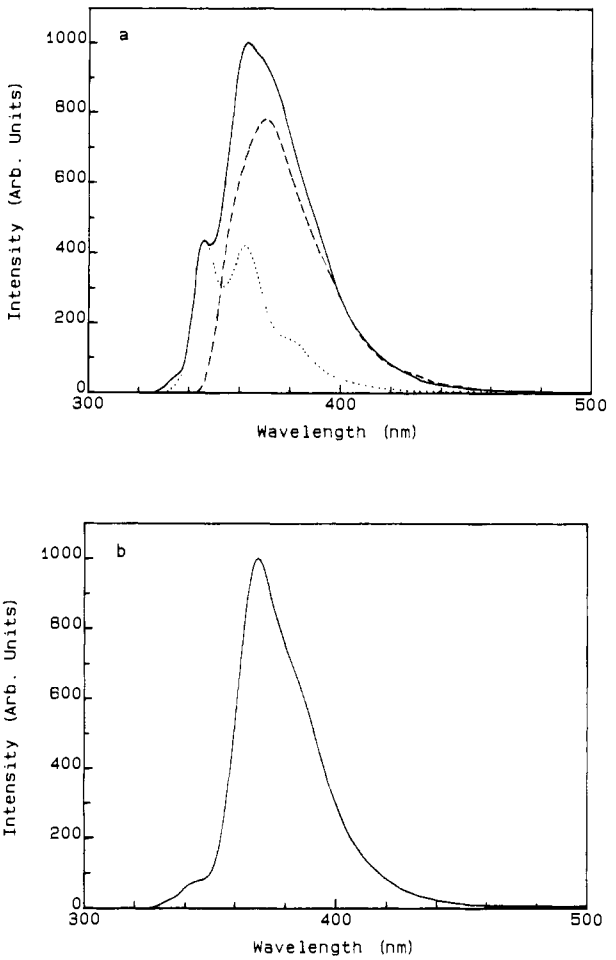

Figure 4. (a) Normalized (at 347 nm) emission spectra of *rac*-DNCzPe (—) and NIPCz (---) in isopentane at 298 K and their difference (- - -). (b) Emission spectrum of *rac*-DNCzPe in isopentane at 140 K.

This behavior is explained as follows. The conformational distribution at 140 K in an alkane solvent yields 1% GG and 99% TT conformers. The TT conformation is the precursor of the TT excimer (partial overlap, Figure 1a,c). The second excimer is thus formed without a rotation of 120° around a carbon–carbon bond of the chain. Only a small rotation (<20°) gives the partial overlap excimer. Further rotation to a full overlap of the chromophores is sterically impossible (Figure 1). The activation energy on the second excimer formation in solution is thus very low because no real energy barrier exists between the TT ground-state conformation and the TT excimer conformation. The activation energy reported by Evers et al.[6] on the second excimer formation is not the activation energy on the second excimer formation in solution but the activation energy on the second excimer formation in a solid matrix.

At higher temperatures (above 140 K) the distribution of the ground-state conformations changes according to the Boltzmann law. For example, at room temperature, in deuterated octane solution, there are about 89% TT conformers and 11% GG conformers in the ground state. Excitation leads to 89% TT locally excited state conformers which form very rapidly (<100 ps)[7] the TT excimer, with an emission maximum at 370 nm, and to 11% GG locally excited state conformers, with emission maxima at 347 and 365 nm. No indication was found of "normal excimer" emission at 420 nm. This is due to the fact that all TT excited states are captured in the second excimer, and that it takes one easy rotation and one hindered rotation to form the TḠ conformation (total overlap of the chromophores) from the GG excited state. The excited-state kinetics in *rac*-DNCzPe are represented in Scheme I. It is evident that no information about the dissociation of the second excimer can be obtained from stationary-state measurements, because on the basis of the data it is not possible

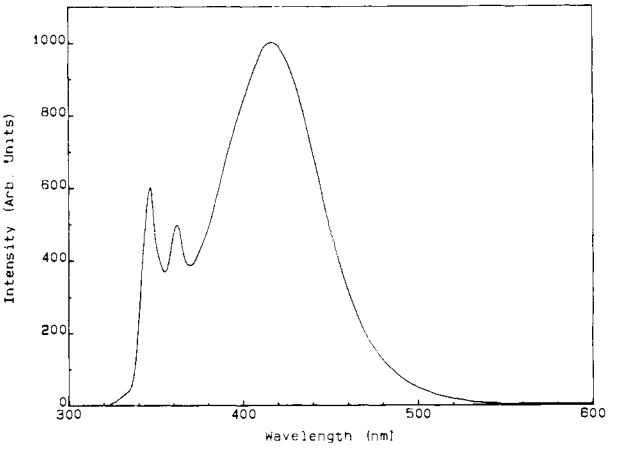

Figure 5. Emission spectrum of *meso*-DNCzPe in isooctane at 298 K.

Scheme I. Excimer Formation in *rac*-DNCzPe

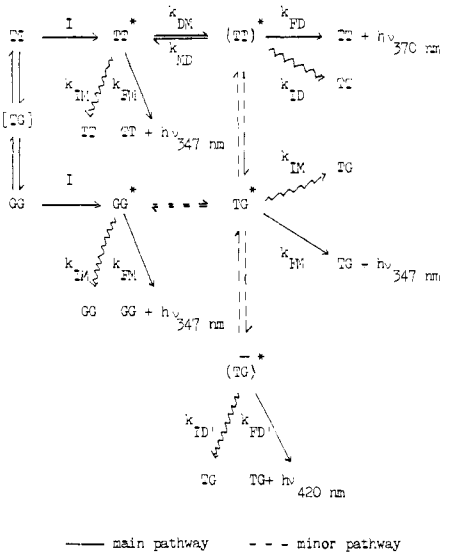

to know whether or not the GG conformation forms the second excimer.

The fluorescence spectrum of *rac*-DNCzPe was also taken in a series of alkane solvents with increasing viscosity. No change in the ratio of the fluorescence intensities at 347 and 370 nm was observed when the solvent was changed from decane to hexadecane. A slight decrease of the emission intensity at 347 nm is observed in isooctane and isopentane. The change, however, is very small (<2%). This corroborates the suggestion that a small change in spatial arrangement of the chromophores is sufficient to form the second excimer.

The fluorescence spectrum of *meso*-DNCzPe in isooctane at room temperature is given in Figure 5. The emission spectrum consists of structured *N*-alkylcarbazole emission and a broad intense emission band with maximum at 420 nm. The emission at 420 nm is ascribed to excimer emission from a total overlap excimer, namely, the "normal" excimer (Figure 2). More information about the excimer formation in *meso*-DNCzPe is obtained by a temperature-dependence study of the fluorescence spectrum in isooctane. At low temperatures the dominant emission is due to the locally excited state. When the temperature is raised the excimer emission becomes more and more important and an isoemissive point is detected. Above 320 K the excimer emission diminishes again in comparison with the locally excited state emission. This behavior can be described by the kinetic Scheme II. Besides the decrease of the excimer emission intensity at higher temperatures a slight hypsochromic shift of the excimer emission maximum is observed. This shift of the maximum can be explained by the change of the population of higher vibronic and rotational levels in the excimer. The conformational distribution

Scheme II. Excimer Formation in *meso*-DNCzPe

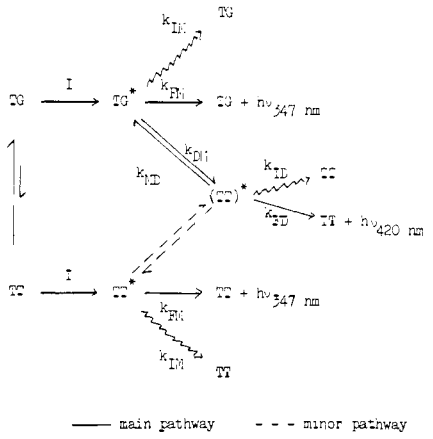

of the ground state in the temperature region studied (180–350 K) is within experimental error 100% TG, and upon excitation at 320 nm an isolated chromophore is excited. The excimer with total overlap of the chromophores (TT) is formed via one rotation of the chain backbone. When the TT conformation is excited, excimer is formed immediately. The formation of the $\bar{G}\bar{G}$ excimer cannot be excluded, but it is less likely formed on the basis of energetic considerations. No indication of the second excimer formation was found in the whole temperature range studied for *meso*-DNCzPe in solution. The ratio of the quantum yield for excimer emission Φ_E and quantum yield for locally excited state emission Φ_M assuming Scheme II and with 100% TG ground-state conformations at the temperatures studied is given by eq 2. At

$$\frac{\Phi_E}{\Phi_M} = \frac{k_{FD}}{k_{FM}} \frac{k_{DM}}{k_{MD} + k_{FD} + k_{ID}} \tag{2}$$

low temperatures where $k_{MD} << (k_{FD} + k_{ID})$ eq 2 simplifies to eq 3. The slope of ln (Φ_E/Φ_M) vs. $1/T$ equals the difference

$$\frac{\Phi_E}{\Phi_M} = \frac{k_{FD}}{k_{FM}} \frac{k_{DM}}{k_{FD} + k_{ID}} \tag{3}$$

between the activation energy on k_{DM} and $(k_{FD} + k_{ID})$. As the activation energy on $(k_{FD} + k_{ID})$ is usually small compared with the activation energy on k_{DM}, the activation energy for the excimer formation is found. For *meso*-DNCzPe in isooctane this activation energy is 15.9 kJ mol^{-1}. The so-called high-temperature region where k_{MD} becomes large in comparison with $(k_{FD} + k_{ID})$ is reached at 350 K. An accurate determination of the enthalpy of excimer formation of *meso*-DNCzPe in isooctane was not possible, since the high-temperature region is reached at 350 K. Kinetic and thermodynamic parameters of excimer formation in *meso*-DNCzPe were obtained by the use of the time-resolved single-photon counting technique (vide infra).

The fluorescence spectrum of DNCzPr in isooctane is shown in Figure 6. This spectrum was reported before.[1c] The measurements on DNCzPr were done in view of a reinterpretation of the kinetics of excimer formation in function of the starting conformations present in the ground state. Morawetz[24] assumes the presence of several conformations in the intramolecular excimer formation in compounds of the type $ArCH_2XCH_2Ar$ where Ar is phenyl, 1-naphthyl, or 4-biphenyl and X is CH_2, O, $N^+(CH_3)_2$, or $NCOCH_3$. The rate constant of the excited-state complex formation k_{obsd} is set equal to fk_a, where f is the fraction of monomer in a conformation from which a single hindered rotation can lead to excimer formation. k_a is the rate constant of the rotation from the trans-gauche$^{\pm}$ conformation to the gauche$^{\mp}$-gauche$^{\pm}$ conformation of the excimer. A kinetic scheme which takes into account the ground-state conformations in DNCzPr is given in Scheme III.

(24) Goldenberg, M.; Emert, J.; Morawetz, H. *J. Am. Chem. Soc.* **1978**, *100*, 7172.

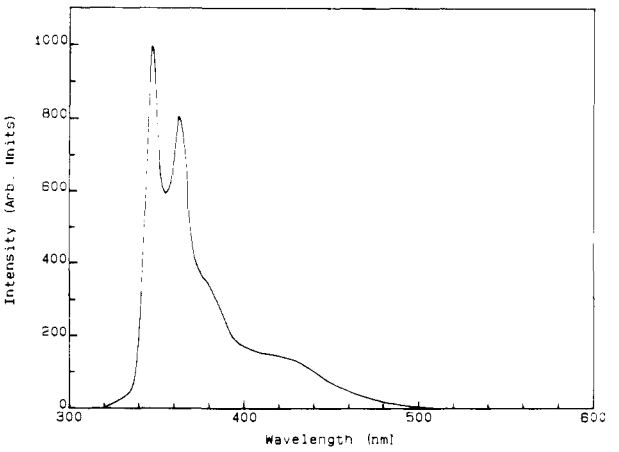

Figure 6. Emission spectrum of DNCzPr in isooctane at 298 K.

Scheme III. Excimer Formation in DNCzPr

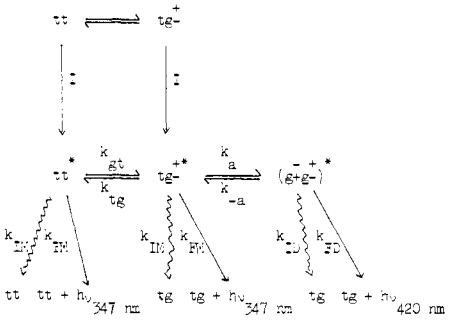

More information about the excimer formation in DNCzPr is obtained by a temperature study of the fluorescence spectrum of DNCzPr in isooctane. Thermodynamic and kinetic data of DNCzPr in methyltetrahydrofuran were reported before by Johnson,[25] but the results were interpreted without taking into account the conformational distribution in the ground state. At low temperatures the emission consists of predominantly locally excited state emission. When the temperature is raised an increase of the excimer emission and a decrease of the locally excited state emission is observed. At 310 K a maximum is reached for the intensity ratio of the excimer over the locally excited state emission. Further increasing the temperature leads to a decrease of the excimer emission intensity and increase of the locally excited state emission intensity. Besides this decrease of the excimer emission intensity a slight hypsochromic shift of the excimer emission maximum is observed comparable with the shift observed for the excimer in *meso*-DNCzPe. A consequence of this observation is the necessity of using quantum yields instead of intensities when ln (Φ_E/Φ_M) is plotted vs. $1/T$. The value of $\Delta H°$ obtained by Johnson[25] is thus inaccurate. The data of DNCzPr in isooctane were analyzed within the framework of Scheme III. Two possibilities are considered:

When the rate of excimer formation is rate determining and the first equilibrium is established rapidly, Scheme III reduces in essence to an intramolecular analogue of the scheme proposed by Birks.[25,26] The rate constant of excimer formation at every temperature will be fk_a. Values of f at any temperature can be calculated when $\Delta G°$ between the ground-state conformations tt and tg$^{\pm}$ is known.

If the rate constant of rotation from tt to tg$^{\pm}$ (k_{gt}) in the excited state is comparable to the rate constant of excimer formation (k_a) other equations are used.[27] The ratio of the quantum yields of excimer emission (Φ_E) over the locally excited state emission (Φ_M) is then given by eq 4. f_{tg} is the fraction of molecules originally

$$\frac{\Phi_E}{\Phi_M} = \frac{k_{FD}}{k_{FM}} \frac{k_a}{k_{1D} + k_{FD}} \frac{k_{gt} + f_{tg}(k_{FM} + k_{1M})}{k_{FM} + k_{1M} + k_{gt} + f_{tt}k_a} \tag{4}$$

(25) Johnson, G. E. *J. Chem. Phys.* **1974**, *61*, 3002.

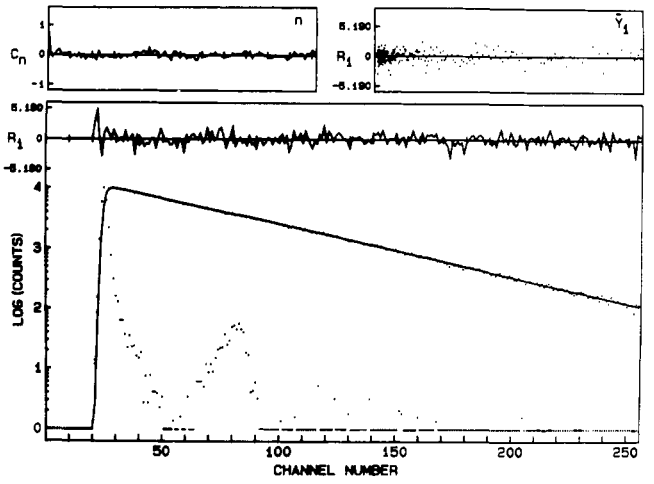

Figure 7. Emission-decay curve of *meso*-DNCzPe in isooctane at 183 K. λ_{exc} = 300 nm; λ_{an} = 347 nm; channel width = 0.246 ns; χ^2 = 1.06; D = 1.87; R_i between −2 and 2 = 96%; $1/\lambda_2$ = 12.1 ns.

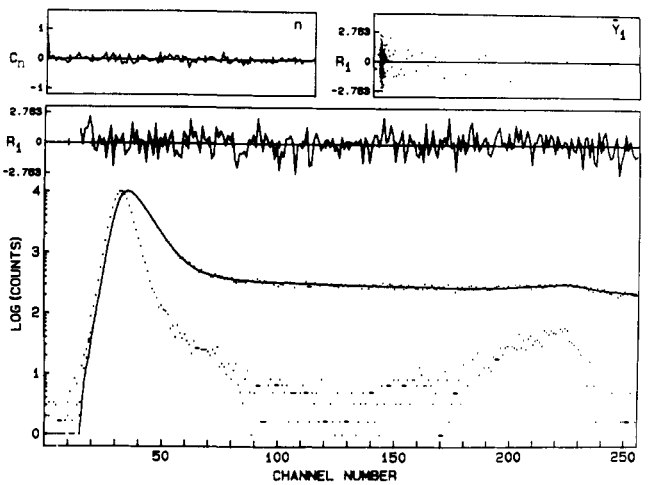

Figure 8. Emission-decay curve of *meso*-DNCzPe in isooctane at 298 K. λ_{exc} = 300 nm; λ_{an} = 347 nm; channel width = 0.074 ns; χ^2 = 1.07; D = 2.03; R_i between −2 and 2 = 95%; $1/\lambda_2$ = 0.430 ns; $1/\lambda_1$ = 36.4 ns.

in the tg± conformation; f_{tt} is the fraction of the molecules in the tt conformation ($1 - f_{tg}$). This equation holds when $k_{-a} << (k_{FD} + k_{ID})$ and $k_{tg} << (k_a + k_{FM} + k_{IM})$ (low-temperature region). At temperatures where $k_a f_{tt} > (k_{IM} + k_{FM} + k_{gt})$ and $k_{gt} > f_{tg}(k_{FM} + k_{IM})$ the activation energy found is the activation energy of the rotation from tt to tg±. In other conditions the value of the different activation energies cannot be obtained from stationary-state measurements. A distinction between the two possibilities within Scheme III is made when time resolved measurements are discussed (vide infra).

(b) Fluorescence Decay Measurements. It is experimentally not possible to obtain a separate decay curve of the excimer or locally excited state emission of *rac*-DNCzPe in isooctane because of the spectral overlap of these emissions (Figure 4). The decay curves obtained at 347, 370, and 460 nm were analyzed as monoexponentials with decay parameters 16.6, 16.5, and 17.4 ns. Fitting the decay curves to two and three exponential decay functions did not result in a substantial improvement of the fitting statistics. These measurements substantiate the prompt second excimer formation as seen in the transient absorption measurements;[7] i.e., no growing in is observed even at 460 nm. No indication of "normal" total overlap excimer formation was found in the decay curve monitored at 460 nm. The exponential behavior of the decays at 347, 370, and 460 nm are compatible with kinetic Scheme I. The TT conformation forms very rapidly (<100 ps)[7] the second excimer. The decay parameter of this second excimer is 17 ns (±1 ns). The GG conformation (11% in solution at room temperature) does not form the TT excimer nor the total overlap excimer. The decay parameter of this GG conformation will thus be the decay parameter of the monochromophoric model NIPCz. It is obvious that it is difficult to resolve a decay parameter of 14.9 ns and a decay parameter of 17 ns.[15] Whether dissociation of the second excimer occurs cannot be elucidated by these measurements.

The emission of *meso*-DNCzPe in isooctane, monitored at 347 nm, decays monoexponentially at temperatures below 203 K. The decay parameter changes from 12.1 ns at 183 K to 5.3 ns at 198 K. At temperatures above 198 K the decay of the emission of the locally excited state deviates from monoexponentiality, but can be analyzed as a sum of two exponential terms. The fast decay parameter changes from 4.6 ns at 203 K to 0.2 ns at 343 K, the second decay parameter varies between 39.6 and 32.8 ns in the same temperature region. No indication was found of a third exponent as indicated in ref 6. Examples of decay curves of *meso*-DNCzPe in isooctane monitored at 347 nm in the different temperature regions are given in Figures 7 and 8. The emission of *meso*-DNCzPe in isooctane monitored at 460 nm over the whole temperature region cannot be described by a monoexponential decay function. When analyzed as the difference of two exponentials good fits were obtained (Figure 9). The growing-in

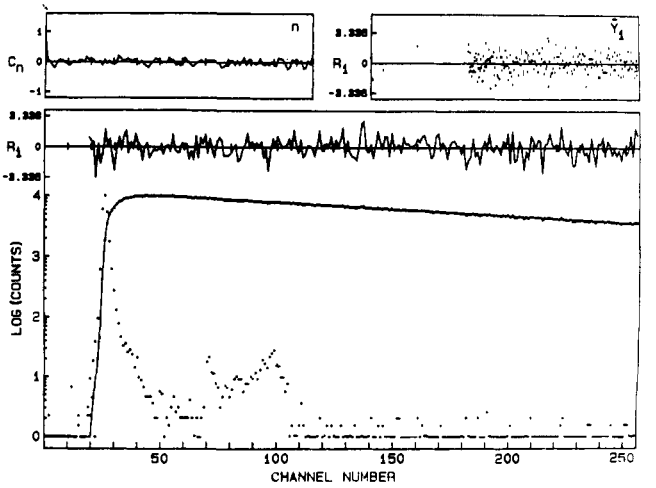

Figure 9. Emission-decay curve of *meso*-DNCzPe in isooctane at 298 K. λ_{exc} = 300 nm; λ_{an} = 460 nm; channel width = 0.187 ns; χ^2 = 1.04; D = 1.94; R_i between −2 and 2 = 95%; $1/\lambda_2$ = 0.540 ns; $1/\lambda_1$ = 36.4 ns.

parameter of the excimer has the same value as the short decay parameter of the locally excited state (at every temperature), the decay parameter has the same value as the long decay parameter of the locally excited state, and the ratio of the preexponential factors equals −1. These observations are consistent with Scheme II. When only the TG ground-state conformation is taken into account—the TT conformation at 393 K is present for only 6%—one can derive the following equations for the decay of the fluorescence intensities of the locally excited state $i_M(t)$ and the excimer $i_E(t)$.[25,26]

$$i_M(t) \sim \frac{k_{FM}}{\lambda_2 - \lambda_1}\{(\lambda_2 - Y)\exp(-\lambda_2 t) + (Y - \lambda_1)\exp(-\lambda_1 t)\} \quad (5)$$

$$i_E(t) \sim \frac{k_{FD}k_{DM}}{\lambda_2 - \lambda_1}\{\exp(-\lambda_1 t) - \exp(-\lambda_2 t)\} \quad (6)$$

with

$$X = k_{FM} + k_{IM} + k_{DM} \qquad Y = k_{FD} + k_{ID} + k_{MD}$$

$$\lambda_{1,2} = \tfrac{1}{2}\{(X + Y) \mp [(X - Y)^2 + 4k_{DM}k_{MD}]^{1/2}\}$$

(26) (a) Förster, Th.; Kasper, K. *Z. Phys. Chem.* (*Wiesbaden*) **1954**, *1*, 275. (b) Förster, Th.; Kasper, F. *Z. Elektrochem.* **1955**, *59*, 976. (c) Stevens, B.; Ban, M. J. *Trans. Faraday Soc.* **1969**, *60*, 1515. (d) Birks, J. B. "Photophysics of Aromatic Macromolecules"; Wiley: New York, 1970. (e) Braun, H.; Förster, Th. *Z. Phys. Chem.* (*Wiesbaden*) **1971**, *78*, 40. (f) Klöpffer, W. "Organic Molecular Photophysics"; Birks, J. B., Ed.; Wiley: New York, 1973; Vol. I. (g) Hui, M. H.; Ware, W. R. *J. Am. Chem. Soc.* **1976**, *98*, 4722.

Table V. Rate Constants and Thermodynamic Data for *meso*-DNCz Pe in Isooctane

$10^{-7}k_{FM}$, s^{-1}	3.1	$10^{-6}k_{FD}$, s^{-1} [a]	4.3
$10^{-7}k_{1M}$, s^{-1}	3.4	$10^{-7}k_{1D}$, s^{-1} [a]	2.2
$E_{(FM+1M)}$, kJ/mol	0	$E_{(FD+1D)}$, kJ/mol	1.6
$10^{-11}k'_{DM}$, s^{-1}	8.3	$10^{-13}k'_{MD}$, s^{-1}	1.4
E_{DM}, kJ/mol	16.0	E_{MD}, kJ/mol	35.8
$-\Delta H°$, kJ/mol	19.8	$-\Delta S°$, J/(mol K)	23.5

[a] Room temperature.

The results of the analysis are presented in Table V.

The fluorescence decay measurements of DNCzPr in isooctane make it possible to distinguish between the two possibilities within Scheme III:

When the values of the rate parameters of the first equilibrium in the excited state in Scheme III are large compared with the values of the rate parameters of the last equilibrium (i.e., the excimer formation is the rate-determining step), Scheme III reduces to an intramolecular analogue of the kinetic scheme of Birks.[25,26] The tt conformation converts rapidly to the tg± conformation in the excited state so that the two conformations (tt and tg±) cannot be distinguished experimentally. The excimer is thus formed from a "pool" of conformations. The fluorescence decay measurements can be analyzed within these assumptions with eq 5 and 6. The observed rate constant of excimer formation k_{obsd} can be written as $f_{tg}k_a$. The observed activation energy will be given by eq 7 where E_a is the activation energy of the excimer

$$E_{obsd} = E_a + \frac{\Delta H°_M}{1 + K_M} \tag{7}$$

formation step, $\Delta H°_M$ is the enthalpy change for the equilibrium between the locally excited states, and K_M is the equilibrium constant of the equilibrium between the locally excited states at temperature T. For values of $\Delta H°_M$ between −0.5 and 0.5 kcal/mol, obtained from other measurements (^{1}H NMR, IR, ...), the correction to be made due to the second term in eq 7 is within experimental error. For values of $\Delta H°_M$ larger than 0.5 kcal/mol or smaller than −0.5 kcal/mol the correction to be made is significant.

When the rate parameters of the first equilibrium in the excited state in Scheme III are of comparable magnitude with the rate parameters of the last equilibrium, the decay functions of locally excited state and excimer fluorescence within Scheme III become more complicated. In the low-temperature region it is assumed that $k_{-a} << (k_{FD} + k_{1D})$ and that $k_{tg} << (k_a + k_{FM} + k_{1M})$.[27] The time evolution of the emission of the locally excited state $i_M(t)$ and of the excimer $i_E(t)$ is given by eq 8 and 9 with $k_M = k_{1M}$

$$i_M(t) \sim f_{tt}\left(1 + \frac{k_{gt}}{k_a - k_{gt}}\right)\exp[-(k_{gt} + k_{FM} + k_{1M})t] + \left(f_{tg} - \frac{f_{tt}k_{gt}}{k_a - k_{gt}}\right)\exp[-(k_a + k_{FM} + k_{1M})t] \tag{8}$$

$$i_E(t) \sim \frac{f_{tt}k_{gt}}{k_M + k_{gt} - k_D} + \frac{f_{tg}k_a - k_{gt}}{k_M + k_a - k_D}\exp(-k_D t) + \frac{f_{tg}k_a - k_{gt}}{k_D - k_a - k_M}\exp[-(k_M + k_a)t] + \frac{f_{tg}k_{gt}}{k_D - k_a - k_M}\exp[-(k_M + k_{gt})t] \tag{9}$$

$+ k_{FM}$ and $k_D = k_{1D} + k_{FD}$. A distinction between the two possibilities within Scheme III is thus possible when decays of the locally excited state are analyzed in the low-temperature region.

The emission of DNCzPr in isooctane, monitored at 347 nm, decays monoexponentially at temperatures below 213 K (Figure 10). Fitting the decay curves to two and three exponential decay functions gives no improvement of the fitting statistics. The emission decay of DNCzPr in isooctane, monitored at 347 nm, can be described adequately by a sum of two exponential terms at temperatures above 213 K (Figure 11). The emission of DNCzPr in isooctane, monitored at 460 nm, decays as the difference of two exponential terms (Figure 12). The short decay parameter observed at 347 nm has the same value as the grow-

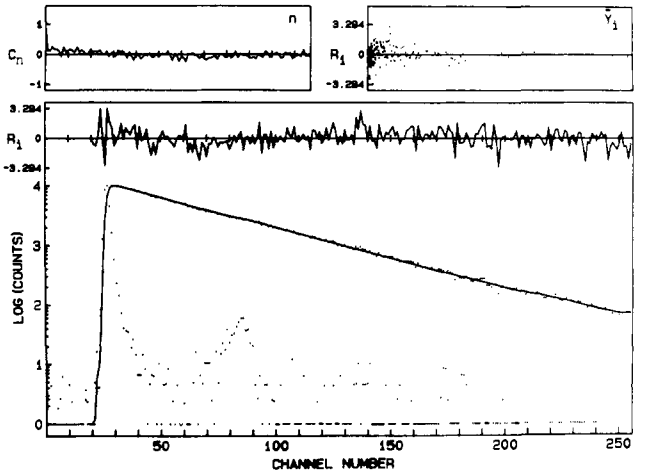

Figure 10. Emission-decay curve of DNCzPr in isooctane at 203 K. λ_{exc} = 300 nm; λ_{an} = 347 nm; channel width = 0.233 ns; χ^2 = 1.03; D = 1.79; R_i between −2 and 2 = 95%; $1/\lambda_2$ = 9.4 ns.

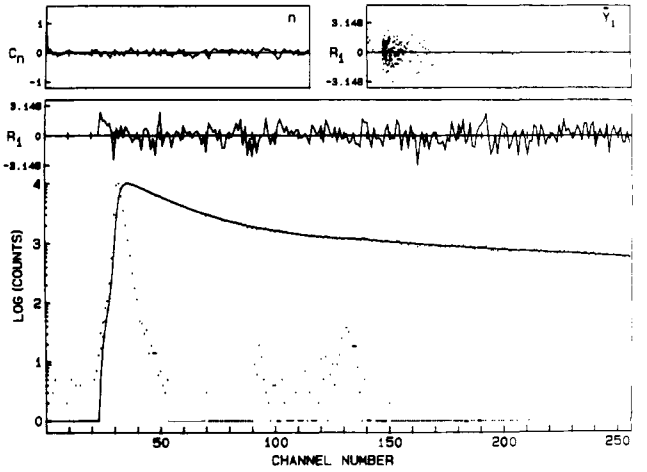

Figure 11. Emission-decay curve of DNCzPr in isooctane at 298 K. λ_{exc} = 300 nm; λ_{an} = 347 nm; channel width = 0.142 ns; χ^2 = 1.01; D = 1.86; R_i between −2 and 2 = 97%; $1/\lambda_2$ = 2.7 ns; $1/\lambda_1$ = 27.9 ns.

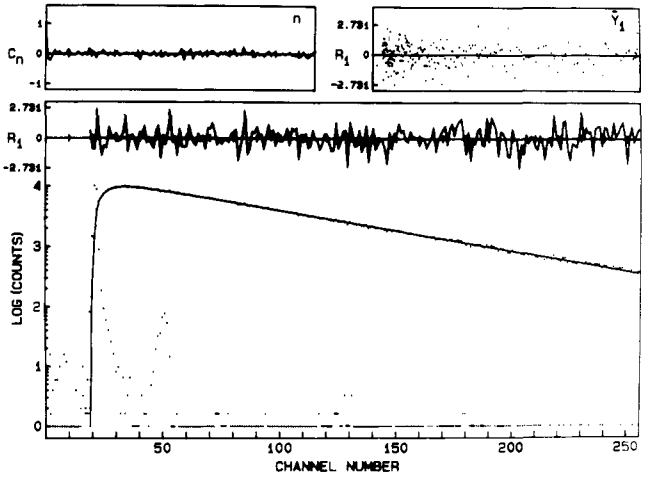

Figure 12. Emission-decay curve of DNCzPr in isooctane at 298 K λ_{exc} = 300 nm; λ_{an} = 460 nm; channel width = 0.488 ns; χ^2 = 0.99; D = 2.00; R_i between −2 and 2 = 95%; $1/\chi_2$ = 2.7 ns; $1/\lambda_1$ = 31.4 ns.

(27) Van der Auweraer, M.; Gilbert, A.; De Schryver, F. C. *J. Am. Chem. Soc.* **1980**, *102*, 4007.

Table VI. Rate Constants and Thermodynamic Data for DNCzPr in Isooctane

$10^{-7}k_{FM}$, s^{-1}	3.1	$10^{-6}k_{FD}$, s^{-1} [a]	3.7
$10^{-7}k_{IM}$, s^{-1}	3.4	$10^{-7}k_{ID}$, s^{-1} [a]	2.6
$E_{(FM+IM)}$, kJ/mol	0	$E_{(FD+ID)}$, kJ/mol	1.6
$10^{-11}k'_{obsd}$, s^{-1}	2.3	$10^{-13}k'_{-a}$, s^{-1}	5.7
E_{obsd}, kJ/mol	16.4	E_{-a}, kJ/mol	34.9
$-\Delta H°$, kJ/mol	18.5	$-\Delta S°$, kJ/(mol K)	45.8

[a] Room temperature.

ing-in parameter observed at 460 nm at all temperatures. The long decay parameter observed at 347 nm at all temperatures above 213 K has the same value as the decay parameter observed at 460 nm. These measurements lead to the conclusion that the first possibility within Scheme III, where a fast preequilibrium exists between the locally excited state conformations, can be used for the analysis of the data. The results of the analysis are given in Table VI. It is important to notice that the rate constant of excimer formation, the activation energy of the excimer formation, and the enthalpy and entropy change in the excimer formation step are the values as observed. A correction for the observed values could not be made since no exact information is known about the first equilibrium between the locally excited state conformations.

Conclusions

^{1}H NMR measurements on model systems for poly(*N*-vinylcarbazole) were performed in order to obtain information about the ground-state conformational distribution in these model systems. It is shown that the knowledge of the ground-state conformations and their population is a necessary basis for the interpretation of the photophysical behavior of the model systems.

The 2,4-di-*N*-carbazolylpentanes are better model systems than 1,3-di-*N*-carbazolylpropane for the description of the photophysical processes in poly(*N*-vinylcarbazole). *meso*-DNCzPe is the model for the isotactic dyad in the polymer and *rac*-DNCzPe is the model for the syndiotactic dyad in the polymer. The results prove that any scheme representing a direct equilibrium between the two excimers is not valid. On the other hand, the conformational distribution of a dyad in the polymer is different from the conformational distribution in the corresponding model. Theoretical calculations[28] indicate a higher population of the TT conformation in the syndio- and isotactic dyads. This means that the excimer formation in the isotactic dyad will differ from the excimer formation in *meso*-DNCzPe since for the latter no indication of a contribution of the TT conformation is found in the ^{1}H NMR measurements. The TT conformation in the isotactic dyad will form very rapidly the "normal" excimer. The experimental data on the pentane models prove the necessity to consider the different behavior of the dyads and the ground-state conformational distribution within the two dyads when the photophysical behavior of the polymer is discussed. In a general case for every dyad there will be two conformations populated in the ground state. It is clear that excimer formation from four different species, with the possibility of more than one type of excimer species, leads to a complex photophysical behavior. One should notice that pentane model systems are not capable of giving information about energy migration along the polymer chain. This phenomenon, if present, will form an additional difficulty in the analysis of polymer photophysics.[29]

The influence of various solvents on the conformational distribution and hence on the excimer formation as well as the influence of the solvent viscosity on the excimer formation will be reported separately.[30]

Acknowledgment. We thank the FKFO and the University Research Fund for financial support to the laboratory. J.V. thanks the IWONL for a predoctoral fellowship. N.B. is a Research Associate of the National Fund for Scientific Research. H.M. is grateful to the University Research Fund for a research fellowship.

Appendix

Derivation of Equation 7. In this derivation, Scheme III is assumed. A fast equilibrium is present in the excited state between the locally excited state conformations:

$$k_{obsd} = f_{tg}k_a \tag{10}$$

with

$$f_{tg} = K_M/(1 + K_M)$$

Writing k_{obsd} and k_a in the Arrhenius form transforms eq 10 into eq 11.

$$k'_{obsd}\exp(-E_{obsd}/(RT)) = \frac{K_M}{1 + K_M}k'_a\exp(-E_a/(RT)) \tag{11}$$

When the natural logarithm of eq 11 is taken, and after differentiation with respect to the temperature, eq 7 results.

Registry No. DNCzPr, 25837-66-5; *meso*-DNCzPe, 80039-86-7; *rac*-DNCzPe, 80039-85-6.

(28) Sundararajan, P. R. *Macromolecules* **1980**, *13*, 512.

(29) Fredrickson, G. H.; Frank, C. W. *Macromolecules* **1983**, *16*, 572.

(30) Vandendriessche, J.; Palmans, P.; De Schryver, F. C.; Boens, N., unpublished results.